Metal immobilization by sludge-derived biochar: roles of mineral oxides and carbonized organic compartment

Weihua Zhang, Xinchen Huang, Yanming Jia, Frédéric Rees, Daniel C. W. Tsang, Rongliang Qiu, Hong Wang

Environ Geochem Health
DOI 10.1007/s10653-016-9851-z

ORIGINAL PAPER

Metal immobilization by sludge-derived biochar: roles of mineral oxides and carbonized organic compartment

Weihua Zhang · Xinchen Huang · Yanming Jia · Frederic Rees · Daniel C. W. Tsang · Rongliang Qiu · Hong Wang

Received: 25 January 2016 / Accepted: 5 July 2016

Abstract Pyrolyzing sludge into biochar is a potentially promising recycling/disposal solution for municipal wastewater sludge, and the sludge-derived biochar (SDBC) presents an excellent sorbent for metal immobilization. As SDBC is composed of both mineral oxides and carbonized organic compartment, this study therefore compared the sorption behaviour of Pb and Zn on SDBC to those of individual and mixture of activated carbon (AC) and amorphous aluminium oxide (Al_2O_3). Batch experiments were conducted at 25 and 45 °C, and the metal-loaded sorbents were artificially aged in the atmosphere for 1–60 days followed by additional sorption experiments. The Pb sorption was generally higher than Zn sorption, and the co-presence of Pb reduced Zn sorption on each studied sorbent. Higher sorption capacities were observed at 45 °C than 25 °C for SDBC and AC, while the opposite was shown for Al_2O_3, indicating the significance of temperature-dependent diffusion processes in SDBC and AC. Nevertheless, metal sorption was more selective on Al_2O_3 that showed a greater affinity towards Pb over Zn under competition, correlating with the reducible fraction of sequential extraction. Furthermore, significant amounts of Pb and Zn were additionally sorbed

Electronic supplementary material The online version of this article (doi:10.1007/s10653-016-9851-z) contains supplementary material, which is available to authorized users.

W. Zhang · X. Huang · Y. Jia · R. Qiu
School of Environmental Science and Engineering, Sun Yat-sen University, Guangzhou 510275, China

W. Zhang · R. Qiu
Guangdong Provincial Key Laboratory of Environmental Pollution Control and Remediation Technology, Guangzhou 510275, China

F. Rees
Laboratoire Sols et Environnement, UMR 1120, Université de Lorraine, 2, avenue de la Forêt de Haye, TSA 40602, 54518 Vandoeuvre-lès-Nancy cedex, France

F. Rees
Laboratoire Sols et Environnement, UMR 1120, INRA, 2, avenue de la Forêt de Haye, TSA 40602, 54518 Vandoeuvre-lès-Nancy cedex, France

D. C. W. Tsang
Department of Civil and Environmental Engineering, Hong Kong Polytechnic University, Hung Hom, Kowloon, Hong Kong, China

H. Wang (✉)
School of Environmental Science and Engineering, Southern University of Science and Technology, Shenzhen 518055, China
e-mail: wangh6@mail.sustc.edu.cn

Published online: 18 July 2016

on SDBC following 30-day ageing. The X-ray diffraction revealed the formation of metal-phosphate precipitates, while the X-ray photoelectron spectroscopy showed a larger quantity of metal–oxygen bonding after 30-day ageing of metal-loaded SDBC. The results may imply favourable long-term transformation and additional sorption capacity of SDBC. In conclusion, SDBC resembles the sorption characteristics of both organic and mineral sorbents in different aspects, presenting an appropriate material for metal immobilization during soil amendment.

Keywords Metal sorption · Sludge-derived biochar · Mineral oxides · Activated carbons

Introduction

Compared to direct application of dewatered sludge in farmland, pyrolyzing sewage sludge into biochar is considered as a potentially excellent strategy for sludge recycling/disposal and carbon subtraction (Liu et al. 2014; Song et al. 2014; Wesenbeeck et al. 2014; Kuppusamy et al. 2016). More importantly, the sludge-derived biochar (SDBC) have been found capable of immobilizing different kinds of heavy metal species such as cationic Pb/Zn and oxy-anionic Cr(VI)/As(III) (Lu et al. 2012; Zhang et al. 2013, 2015; Inyang et al. 2016). Contrary to the biochars produced from plant residues (e.g. raw straw and wood strips, Chen et al. 2012) and animal manure (e.g. cattle manure and poultry manure, Cao and Harris 2010), SDBC contains a lower content of organic carbon but a higher content of mineral oxides (Zhang et al. 2013).

The mineral oxides originate from colloids in municipal wastewater are entrapped in sewage sludge, especially when primary sedimentation tank is absent from wastewater treatment process due to the low chemical oxygen demand of the wastewater. These colloids are natural soil components and mainly present as amorphous mineral oxides, thus presenting the bulk of active sites of SDBC. A number of research studies have reported successful metal stabilization by these mineral oxides, such as aluminium oxides (Hovsepyan and Bonzongo 2009), ferric oxides (Komárek et al. 2013) and manganese oxides (Zaman et al. 2009). Besides, the carbonized organic components of biochars accommodate a range of functional groups for metal species in the solution (Tong et al. 2011; Rees et al. 2014). Both carbonized organic components and inorganic mineral oxides should be considered for metal immobilization by SDBC (Qian and Chen 2013), where heterogeneous sorption mechanisms may occur depending on multiple surface properties and their association with pollutants.

The dual role of SDBC has been illustrated in recent studies (Qian and Chen 2013; Lu et al. 2012), and SDBC can serve as an effective dual sorbent for cationic metals (Pb^{2+}, Zhang et al. 2013), oxyanions (CrO_4^{2-}, AsO_2^{-}, Zhang et al. 2015), as well as organic pesticides (Zhang et al. 2015; Tan et al. 2015). However, the individual roles of mineral oxides and carbonized organic compartments are not elucidated; in particular, their corresponding sorption kinetics and dependence on environmental conditions are yet to be figured out. Therefore, activated carbons (AC) and active aluminium oxides (Al_2O_3) were selected as the representative carbonized organic compartment and mineral oxide, respectively, on which Pb and/or Zn sorption was compared to those on SDBC to identify the underlying mechanisms.

In addition, previous studies found that ageing processes may have a significant influence on the metal sorption behaviour (Eick et al. 1999; Ford et al. 1999). The ageing process after sorption can strengthen metal bonding via microporous diffusion, incorporation induced by re-crystallization, and formation and stabilization of surface precipitates (Rorff et al. 2006). As a result, when applying the SDBC for soil fixation, the ageing process may facilitate the metal immobilization. Therefore, the influence of ageing process on metal sorption on SDBC as well as AC and Al_2O_3 was also investigated, with a focus on the sorption capacity and bonding strength.

Materials and methods

Aluminium oxide, activated carbon, and sludge-derived biochar

Active aluminium oxide (Al_2O_3, HPLC grade) and activated carbon (AC) were bought from Sinopharm Chemical Reagent Ltd Co (Shanghai, China), and their properties are summarized in Table 1. The SDBC used

herein was prepared in an LTKC-6-12 pipe oven (Lantian Instrument limited Corp., Hangzhou, China), full of N_2 at a rate of 5 m^3 h^{-1} to ensure inert conditions. Sequentially, the temperature in the pipe oven rose up to 400 °C at a rate of 20 °C min^{-1} and then maintained for 2 h, which are the optimal conditions for pyrolyzing the dewatered sewage sludge into biochar based on our previous study (Zhang et al. 2013). The used sewage sludge was collected from Lijiao Sewage Treatment Plant in Guangzhou (23°20′N, 113°30′E), where an oxidation ditch process with an average hydraulic retention time of 18 h was employed to remove BOD_5, nitrogen, and phosphorus nutrients without the primary sedimentation process. The details on the sludge pyrolysis and properties of SDBC were given in our previous studies (Zhang et al. 2013, 2015), and the major properties of SDBC are indicated in Table 1. Based on the contents of Al and TOC of SDBC, a mixture of Al_2O_3 and AC (6:4 by mass) was also used to simulate the SDBC behaviour.

Metal sorption experiments

Batch sorption experiments were conducted by mixing 0.1 g of (1) SDBC, (2) AC, (3) Al_2O_3, and (4) mixture of AC and Al_2O_3, respectively, with 25 mL of solutions containing various amounts of $Pb(NO_3)_2$ or $Zn(NO_3)_2$ (0.01–0.5 mmol L^{-1}) on a 160 rpm shaker at 25 or 45 °C for 24 h. The solution pH was recorded, and the suspension was filtered with 0.45-μm poresize PES disposable filters (Jinteng, China). The filtrate was acidified to pH < 2 and stored at 4 °C. The concentrations of dissolved metals were determined by Optima 3000 XL inductively coupled plasma-atomic emission spectrometer (PerkinElmer, USA), based on Method 6010C of USEPA SW-846.

The residual sorbents were subject to further characterization. X-ray photoelectron spectroscopic (XPS) spectra were obtained via scanning the SDBC with an ESCALAB 250 X-ray photoelectron spectroscopy (Thermo-VG Scientific, USA). The existence and crystalline form of chemical precipitates on the sorbent surfaces after sorption were identified using Empyrean X-ray powder diffractometer (XRD) (PANalytical B.V., Holland) equipped with a Cu Kα radiation source worked at 40 kV and 40 mA. The surface structure of the SDBC before and after sorption was analysed by scanning electron microscopy (SEM S-520, Hitachi, Japan) and electron dispersive X-ray analysis (EDX system, INCA 300, Oxford, UK). The EDX system was coupled with SEM using mixed BSE (back scatter electron) combined with LSE (lateral secondary electron) signal detector.

To probe the influence of ageing time on metal immobilization by SDBC, additional batch sorption experiments were conducted, where 0.25 μmol L^{-1} Pb and/or Zn solutions were used with the four sorbents for 24 h at 25 °C with the above-mentioned sorption procedure. Solution was separated by centrifugation and filtration with 0.45-μm filter paper, and the resulting Pb or Zn-loaded sorbents were exposed to ambient air at room temperature for 1–30 days. These artificially "aged" sorbents were then put again into contact with 0.25 μmol L^{-1} Pb and/or Zn solution following the above procedure. The sorption capacity of aged sorbents was calculated from the remaining metal concentration in solution and compared to those

Table 1 Properties of different sorbents

Sorbents	Sludge-derived biochar (SDBC)	Activated carbon (AC)	Aluminium oxide (Al_2O_3)
pH (1:10 in DI water)	7.39 ± 0.08	6.85 ± 0.05	7.31 ± 0.03
BET specific surface (m^2 g^{-1})	34.0	1263	147.1
Elemental content (mg kg^{-1})			
Al	74,252 ± 532	5808 ± 2134	
Fe	36,400 ± 632	559 ± 69	
Organic functional groups (mmol g^{-1})			
Phenolic/hydroxyl	0.175	0.201	Not applicable
Carboxyl	0.310	0.285	
Lactones	0.045	0.112	

of fresh sorbents. All experiments were performed in triplicate.

The associations of Pb and Zn to both fresh and aged sorbents were characterized by traditional sequential extraction scheme (Tessier et al. 1979), categorizing into five fractions: (1) cation-exchangeable, (2) acid extractable, (3) reducible, (4) oxidizable, and (5) residual fractions. The details of the extraction procedures are given in our previous studies (Zhang et al. 2010).

Results

Pb and Zn sorption onto different sorbents

Sorption isotherms of single-metal solutions at 25 °C fitted with Freundlich equation are presented in Fig. 1. Table 2 lists the corresponding sorbed amounts on different sorbents for comparison when the initial [Pb] or [Zn] was fixed at 250 μmol L^{-1}. The Pb sorption capacity was consistently higher than the corresponding Zn sorption capacity for each tested sorbent (SDBC, AC, Al_2O_3, and AC + Al_2O_3), especially for AC. The Pb sorption followed the decreasing order of affinity: AC > AC + Al_2O_3 > SDBC > Al_2O_3. Yet, the Zn sorption showed a different order of affinity: AC + Al_2O_3 > SDBC > Al_2O_3 > AC. The sorption capacity of SDBC for both metals was in between those of the mixture of AC + Al_2O_3 and Al_2O_3 alone.

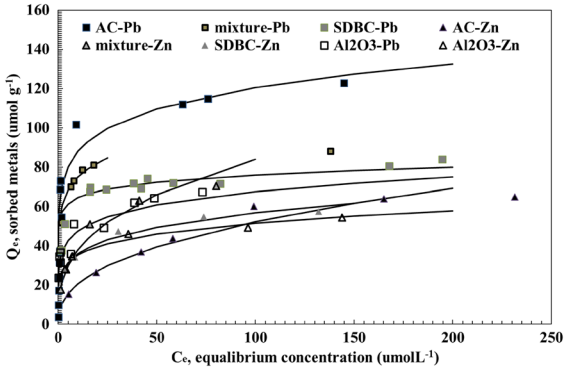

Fig. 1 Pb and Zn sorption isotherms at 25 °C in single-metal solutions on: (a) AC (0.05 g in 50 mL), (b) amorphous Al_2O_3 (0.1 g in 50 mL), (c) mixture of AC and Al_2O_3 (4:6 by mass, 0.1 g in 50 mL), and (d) SDBC (0.1 g in 50 mL) (better fitted by Freudlich equation as shown)

Our preliminary study did not found any detectable Al in the solution in contact with Al_2O_3-containing sorbents (data not shown), eliminating the possibility of Al_2O_3 dissolution and resorption on AC surface. In contrast, SEM image indicated that some Al_2O_3 colloids entered the micropores of AC (as illustrated in the supplementary materials, Fig. S1).

Temperature and metal competition

The results of sorption kinetics at 25 and 45 °C in single-metal and binary-metal solutions of Pb and Zn are presented in Fig. 2. Higher sorption capacities of SDBC and AC were reached at 45 °C than 25 °C. However, for Al_2O_3, higher sorption capacities were observed at 25 °C instead of 45 °C in both single-metal and binary-metal solutions. For the mixture AC + Al_2O_3, there was no difference in sorption at 25 and 45 °C except for Zn sorption in single-metal solution which was higher at 45 °C than 25 °C.

In the sorption isotherms, Pb sorption was consistently higher than Zn sorption, but on SDBC, sorption capacity of Zn was comparable to that of Pb at 45 °C in single-metal solutions. There were higher sorption capacities in single-metal solutions compared to binary-metal solutions. In particular, Zn sorption was decreased by up to 10 times in the presence of Pb, while Pb sorption was only decreased by 10–30 % in the presence of Zn.

Artificial ageing

Additional amounts of Pb and Zn were immobilized on the different sorbents following the ageing process (Fig. 3), with the exception of Zn sorption in binary-metal solutions on AC. The longer the ageing time was, the larger additional amounts of Pb and Zn were sorbed on Al_2O_3 and SDBC. However, there was no conclusive effect of ageing time on AC and AC + Al_2O_3. In particular, a higher amount of Zn was sorbed on AC + Al_2O_3 compared to SDBC at a shorter ageing time, but sorption on SDBC became greater than AC + Al_2O_3 after 30-day ageing.

Sequential extraction results of AC, Al_2O_3, and SDBC before and after 30-day ageing are shown in Fig. 4. For AC, Zn was largely present in the cation-exchangeable fraction and the reducible fraction, while Pb was mainly found in the oxidizable fraction. For Al_2O_3, more than 95 % of Zn sorption was

Table 2 Sorbed amounts of Pb and Zn on different sorbents

System	Metal	Temp (°C)	Amount of sorbed metals (μmol g^{-1})				
			SDBC	Al_2O_3 (1)	AC (2)	AC + Al_2O_3	Combination[a]
Single-metal	Pb	25	75.08	54.00	117.11	79.94	91.86
	Pb	45	82.10	65.96	106.18	80.52	90.09
	Zn	25	48.17	34.26	49.58	61.96	43.45
	Zn	45	79.81	59.35	43.67	80.97	49.94
Binary-metal	Pb	25	50.58	48.52	109.87	64.23	85.33
	Pb	45	65.10	55.40	96.71	62.77	80.19
	Zn	25	7.15	7.83	10.71	12.28	9.56
	Zn	45	10.53	27.29	9.10	11.54	16.37

[a] Calculated by (1) × 0.6 + (2) × 0.4, where initial [Pb] or [Zn] was fixed at 250 μmol L^{-1}

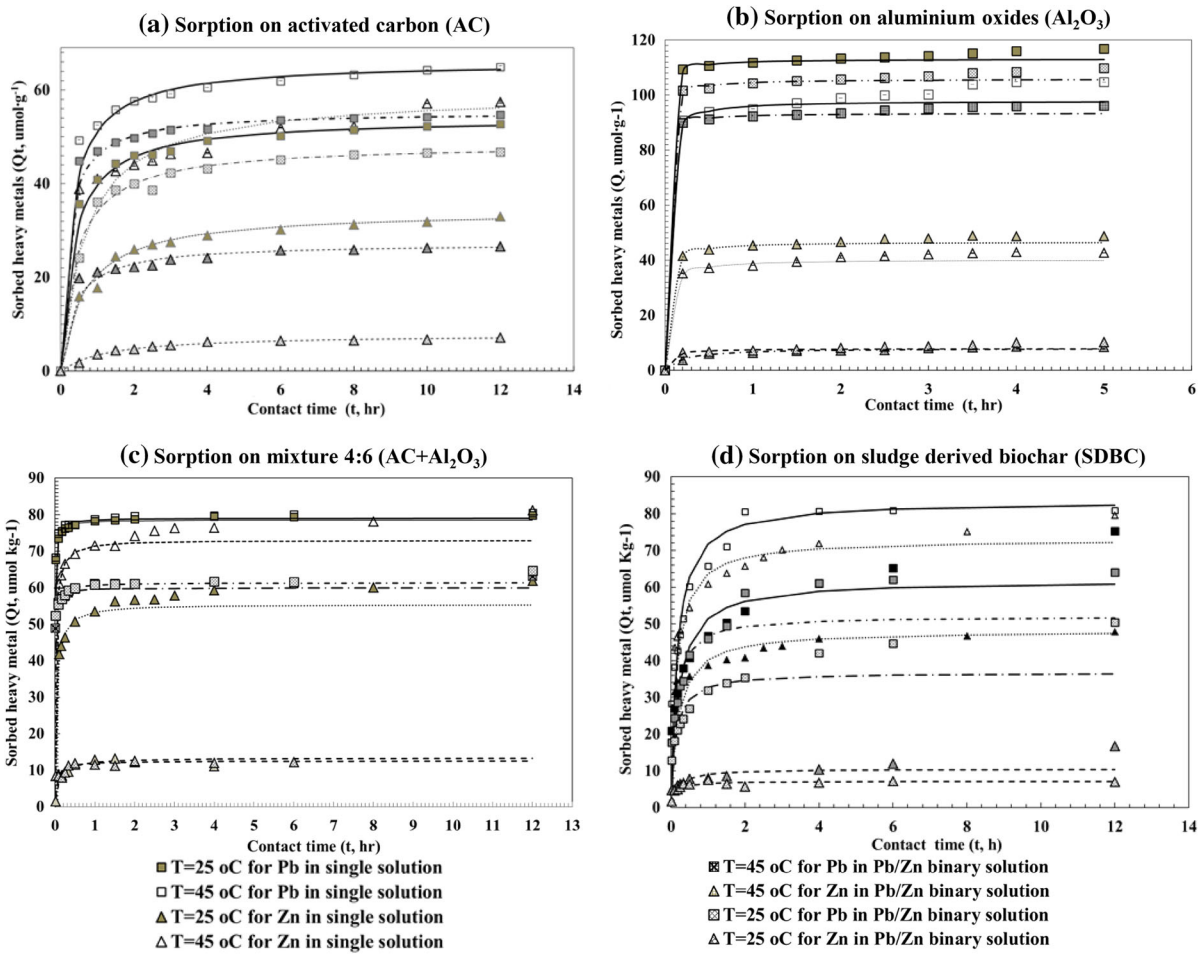

Fig. 2 Pb and Zn sorption kinetics at 25 and 45 °C fitted with second-order kinetic model on: **a** AC (0.05 g in 50 mL), **b** amorphous Al_2O_3 (0.1 g in 50 mL), **c** mixture of AC and Al_2O_3 (4:6 by mass, 0.1 g in 50 mL), and **d** SDBC (0.1 g in 50 mL) (initial [Pb(II)] and [Zn(II)] were 0.25 mM in both single- and binary-metal solutions)

correlated with the reducible fraction, whereas Pb in the acid extractable fraction and the oxidizable fraction were equal or higher than the reducible fraction. For SDBC, oxidizable and residual fractions represented more than 75 % of the Pb sorption while the cation-exchangeable, acid extractable, and

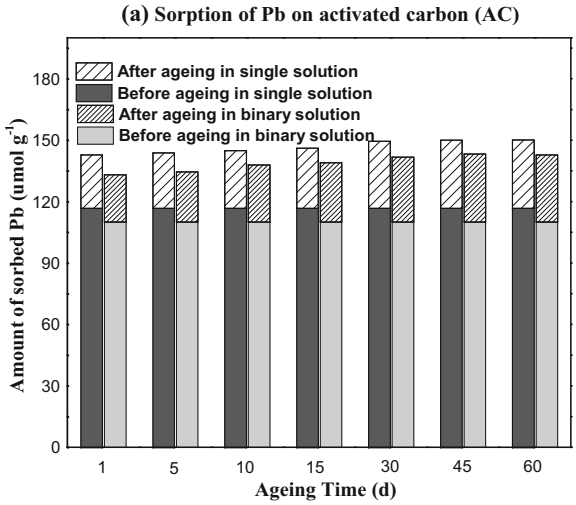
(a) Sorption of Pb on activated carbon (AC)
After ageing in single solution
Before ageing in single solution
After ageing in binary solution
Before ageing in binary solution
Amount of sorbed Pb (umol g-1)
Ageing Time (d)

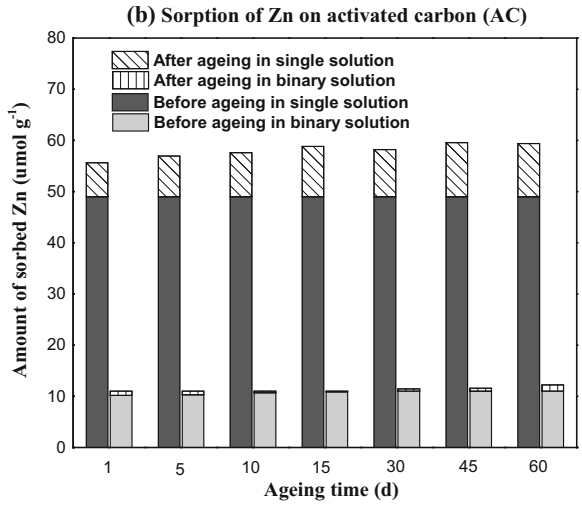
(b) Sorption of Zn on activated carbon (AC)
After ageing in single solution
After ageing in binary solution
Before ageing in single solution
Before ageing in binary solution
Amount of sorbed Zn (umol g-1)
Ageing time (d)

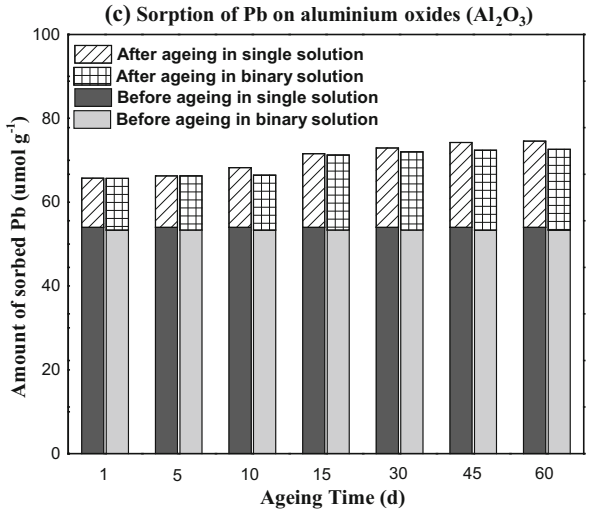
(c) Sorption of Pb on aluminium oxides (Al2O3)
After ageing in single solution
After ageing in binary solution
Before ageing in single solution
Before ageing in binary solution
Amount of sorbed Pb (umol g-1)
Ageing Time (d)

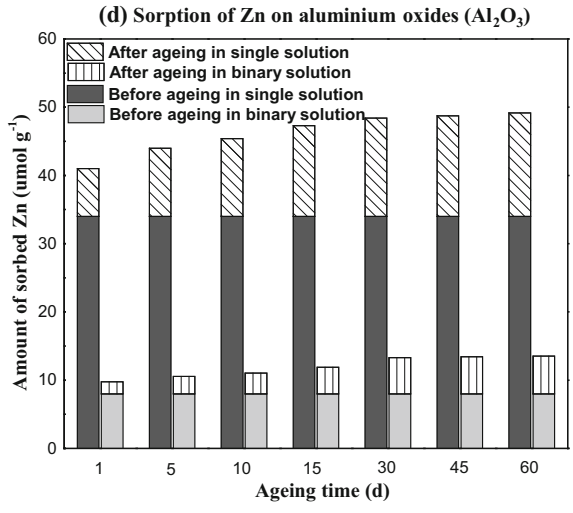
(d) Sorption of Zn on aluminium oxides (Al2O3)
After ageing in single solution
After ageing in binary solution
Before ageing in single solution
Before ageing in binary solution
Amount of sorbed Zn (umol g-1)
Ageing time (d)

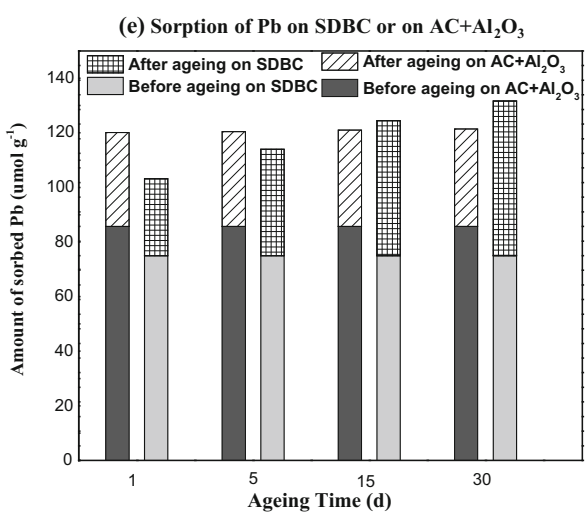
(e) Sorption of Pb on SDBC or on AC+Al2O3
After ageing on SDBC
After ageing on AC+Al2O3
Before ageing on SDBC
Before ageing on AC+Al2O3
Amount of sorbed Pb (umol g-1)
Ageing Time (d)

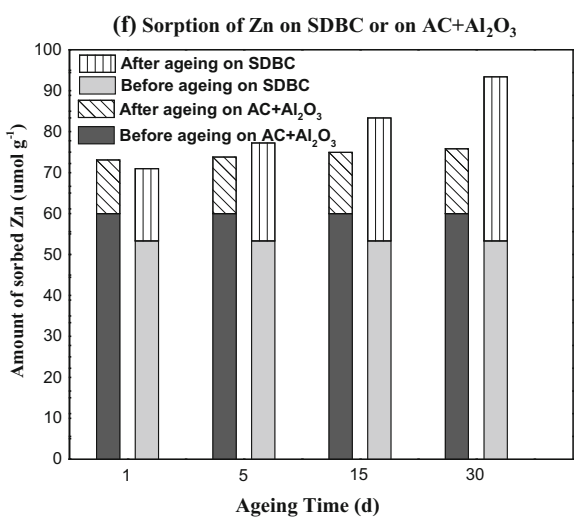
(f) Sorption of Zn on SDBC or on AC+Al2O3
After ageing on SDBC
Before ageing on SDBC
After ageing on AC+Al2O3
Before ageing on AC+Al2O3
Amount of sorbed Zn (umol g-1)
Ageing Time (d)

◀**Fig. 3** Metal sorption on different sorbents after varying artificial ageing time: **a** Pb sorption on AC (0.05 g in 50 mL), **b** Zn sorption on AC (0.05 g in 50 mL), **c** Pb sorption on amorphous Al_2O_3 (0.1 g in 50 mL), **d** Pb sorption on amorphous Al_2O_3 (0.1 g in 50 mL), **e** Pb sorption on mixture of AC and Al_2O_3 (4:6 by mass) and SDBC (0.1 g in 50 mL), and **f** Pb sorption on mixture of AC and Al_2O_3 (4:6 by mass) and SDBC (0.1 g in 50 mL) (Initial [Pb(II)] or [Zn(II)] was 0.25 mM in all solutions)

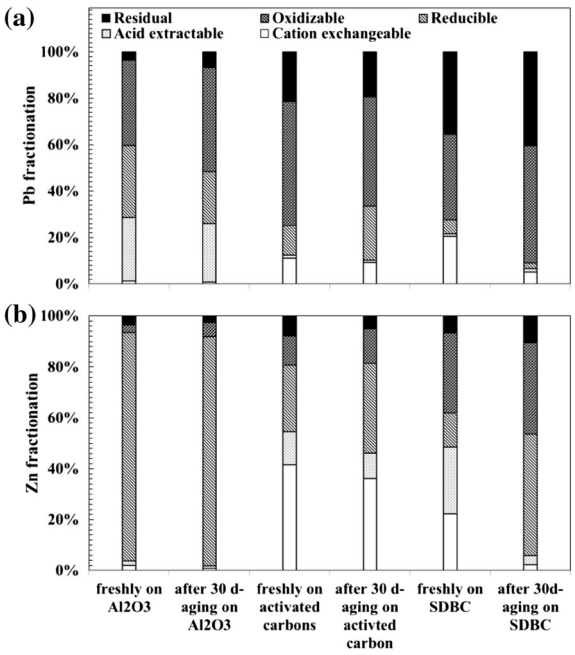

Fig. 4 Sequential extraction of Pb (**a**) and Zn (**b**) sorbed on Al_2O_3, AC, or SDBC, before or after 30-day ageing, respectively

oxidizable fractions accounted for the majority of Zn sorption.

It was found that 30-day ageing had no influence on the distribution of sorbed Zn on Al_2O_3, but resulted in a higher oxidizable fraction and a lower reducible fraction for sorbed Pb. The opposite phenomenon was observed with 30-day ageing of AC, where sorbed Pb was present as a higher reducible fraction and a lower oxidizable fraction but both the reducible and oxidizable Zn increased with less cation-exchangeable fraction. For SDBC, 30-day ageing increased the oxidizable and residual fractions of Pb and decreased the cation-exchangeable and reducible fractions. On the contrary, the reducible fraction of Zn sorbed on SDBC was considerably increased by ageing, while the cation-exchangeable fraction was reduced.

The XRD spectra (as illustrated in the supplementary materials, Fig. S2) proved the existence of crystalline $K_2Pb(PO_3)_4$ on the surface of Pb-loaded SDBC, but they were observed only after 30-day ageing. The XPS O_{1s} spectra (Fig. 5) also showed that 30-day ageing resulted in a larger proportion of M–O (Pb: from 3.85 to 5.71 %; Zn: from 4.19 to 7.18 %), indicating the increased intensity or coverage of Pb/Zn coordination with the oxygen-containing functional groups on the surface of SDBC.

Discussion

Competitive sorption of Pb and Zn

The sorption capacities of each material were higher for Pb than Zn (Fig. 1), which was also commonly observed with organic sorbents (Rees et al. 2014) and inorganic sorbents (Abdus-Salam and Bello 2015). The favourable sorption of Pb compared to Zn (Figs. 1, 2) may be explained by the smaller hydrated ionic radius (4.0 vs. 4.3 Å) and the greater electronegativity of Pb (2.33 vs. 1.65). These would facilitate diffusion of Pb inside micropores and enhance its affinity for cation exchange and surface complexation (Lu and Xu 2009; Depci et al. 2012). In this study, the difference in sorbed amounts of Pb and Zn was greater for AC than SDBC and Al_2O_3 (Fig. 2), possibly reflecting the presence of micropores and non-selective sorption sites. Furthermore, the smaller difference at 45 °C than 25 °C suggested a greater importance of transport processes in AC and SDBC. It was because a higher temperature could accelerate diffusion processes and therefore curtail the preferential sorption of Pb over Zn due to its smaller size.

The Zn sorption (and Pb sorption to a lower extent) was diminished in the binary-metal solutions (Fig. 3), and some sorbed Zn on the aged sorbents was even released due to Pb competition when put in contact with binary-metal solutions again. Similar competitive effects were observed for Pb and Zn in multi-metal solutions (Mohan and Singh 2002; Tsang and Lo 2006; Depci et al. 2012; Rees et al. 2014). This illustrates metal competition for some commonly available sorption sites and electrostatic repulsion of metals with the same charge. The metal fractionation by sequential extraction (Fig. 4) reinforced that Pb was more strongly bound to the sorbents than Zn,

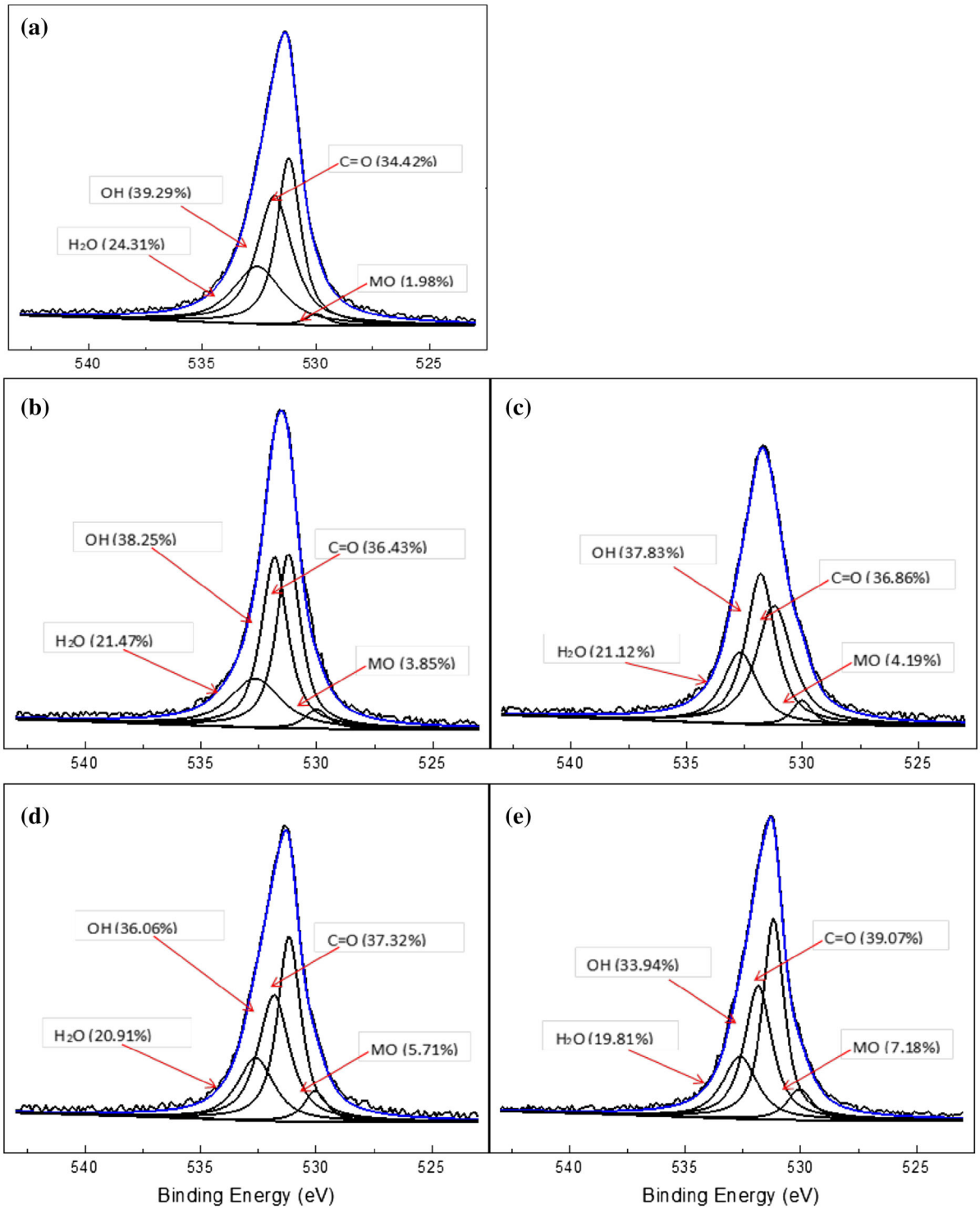

Fig. 5 XPS O_{1s} spectra of SDBC with varying ageing time: **a** original SDBC, **b** freshly Pb-loaded, **c** Pb-loaded after 30-day ageing, **d** freshly Zn-loaded, and **e** Zn-loaded after 30-day ageing

accounting for the greater suppression of Zn sorption by coexisting Pb, but there was only a slight effect vice versa.

Comparison of SDBC with AC and Al_2O_3

The sorption characteristics of SDBC may resemble that of Al_2O_3 (i.e. model mineral sorbent) or that of AC (i.e. model organic sorbent). Despite the contrasting affinity of Pb and Zn for different sorbents, the observed sorption capacities of SDBC were more comparable to those of Al_2O_3 than AC (Figs. 2, 3). The competition of Zn by coexisting Pb was also much stronger for SDBC and Al_2O_3 than AC, suggesting that the mineral components may present sorption sites (e.g. silanol and aluminol groups at the edge or corners) that are characterized by a higher affinity towards Pb than Zn due to difference in their ionic radii and charge densities. The results of sequential extraction (Fig. 4) showed that sorption of Pb and Zn on AC and SDBC took place in all fractions despite with different proportions, while sorption on Al_2O_3 was predominantly on reducible fraction corresponding to mineral oxides.

However, the influence of temperature on metal sorption on SDBC was more similar to that of AC than Al_2O_3 (Fig. 2). An increase in sorption with increasing temperature was seen for SDBC and AC, indicative of an endothermic sorption process (Hefne et al. 2008; Dandanmozd and Hosseinpur 2010). This may correspond to an increase in the kinetic energy or a better solvation of the metal ions (Naseem and Tahir 2001). Similar results of increased sorption capacity and enhanced sorption kinetics on AC at a higher temperature were also reported for Pb (Gueu et al. 2007) and Zn (Marzal et al. 1996). An increase in temperature could facilitate both chemical sorption reactions and physical diffusion processes in SDBC, in a way similar to those in AC. These results reveal that well-recognized diversity of the surface active sites of SDBC plays different roles under varying environmental conditions, i.e. mineral oxides display a more selective sorption under metal competition, whereas carbonized organic compartments are governed by temperature-dependent diffusion processes.

Ageing of sorbed metals

With artificial ageing of metal-loaded SDBC in ambient air, a change was observed in the relative importance of sorption processes. The weaker interactions via cation exchange and coordination with phosphate on SDBC were transformed into crystalline metal precipitates such as $K_2Pb(PO_3)_4$ identified in the XRD spectra after 30-day ageing (as illustrated in the supplementary materials, Fig. S2), suggesting the formation of stronger bonding with mineral oxides and organic matter. This may also explain why ageing led to a higher sorption capacity for all sorbents of this study, particularly for SDBC (Fig. 3), as the transformation of sorbed metals into precipitates may empty previously occupied sorption sites and/or create new reactive surfaces for additional metal sorption from the solution.

In addition, ageing is often associated with the oxidation of biochar surfaces, resulting in a larger quantity of oxygen-containing functional groups that could also lead to a higher sorption capacity via surface complexation (Tsang et al. 2007; Guo et al. 2014). This was confirmed by the XPS spectra (Fig. 5) where the proportions of Pb–O and Zn–O increased with ageing. The sequential extraction (Fig. 4) also revealed a larger oxidizable fraction of Pb on SDBC. On the contrary, this was not observed on AC because the surfaces had already been fully oxidized by the activation process during production. Furthermore, the time-dependent diffusion of metals along the interior surfaces and/or within the small pores of SDBC over time may also contribute to a higher sorption capacity with ageing, although it could not be confirmed in this study.

These beneficial effects of ageing on metal sorption by SDBC implies that the metal immobilization observed in the short term in SDBC-amended soils would probably last longer and become more stable than its sorption capacity measured in batch experiments (Rees et al. 2014; Fang et al. 2016). The slowly releasing metals from contaminated soils may still be sorbed on SDBC over time, yet the resilience of long-term metal immobilization against continuous leaching and varying field conditions (e.g. pH, redox, biotic disturbance) should be further attested (Tsang et al. 2013; Fang et al. 2016).

Conclusions

Pyrolyzing sludge into biochar is a potentially promising recycling/disposal option for the increasing production of municipal wastewater sludge, from which the sludge-derived biochar presents an excellent sorbent for soil amendment because of its abundant contents of carbonized organic and mineral components. This study reveals that sludge-derived biochar can be evaluated as a mixture of activated carbon and aluminium oxide for elucidating the roles of different compartments under different environmental conditions. In particular, sorption on organic compartment is more temperature-dependent due to diffusion processes, while sorption on mineral oxides is more selective under metal competition. Furthermore, ageing of metal-loaded biochar in ambient air results in metal-phosphate precipitation and provides additional sorption sites, implying a favourable long-term effect of SDBC for metal immobilization in soil amendment that requires future investigations.

Acknowledgments The authors wish to thank the National Natural Science Foundation of China (project no. 41272383), and Science and Technology Planning Project of Guangdong Province (2014A050503032) for the financial support of this study.

References

Abdus-Salam, N., & Bello, M. O. (2015). Kinetics, thermodynamics and competitive adsorption of lead and zinc ions onto termite mound. *International Journal Environmental Science and Technology, 12*, 3417–3426.

Cao, X., & Harris, W. (2010). Properties of dairy-manure-derived biochar pertinent to its potential use in remediation. *Bioresource technology, 101*, 5222–5228.

Chen, B., Yuan, M., & Qian, L. (2012). Enhanced bioremediation of PAH-contaminated soil by immobilized bacteria with plant residual and biochar as carriers. *Journal of Soils and Sediments, 12*, 1350–1359.

Dandanmozd, F., & Hosseinpur, A. R. (2010). Thermodynamic parameters of zinc sorption in some calcareous soils. *Journal of American Science, 6*(7), 298–304.

Depci, T., Kul, A. R., & Onal, Y. (2012). Competitive adsorption of lead and zinc from aqueous solution on activated carbon prepared from Van pulp: study in single- and multi-solute systems. *Chemical Engineering Journal, 200*, 224–236.

Eick, M. J., Peak, J. D., Brady, P. V., & Pesek, J. D. (1999). Kinetics of lead adsorption/desorption on goethite: Residence time effect. *Soil Science, 164*, 28–39.

Fang, S., Tsang, D. C. W., Zhou, F., Zhang, W. H., & Qiu, R. L. (2016). Stabilization of cationic and anionic metal species in contaminated soils using sludge-derived biochar. *Chemosphere, 149*, 263–271.

Ford, R. G., Scheinost, A. C., Scheckel, K. G., & Sparks, D. L. (1999). The link between clay mineral weathering and the stabilization of Ni surface precipitates. *Environmental Science and Technology, 33*, 3140–3144.

Gueu, S., Yao, B., Adouby, K., & Ado, G. (2007). Kinetics and thermodynamics study of lead adsorption on to activated carbons from coconut and seed hull of the palm tree. *International Journal Environmental Science and Technology, 4*(1), 11–17.

Guo, Y., Tang, W., Wu, J., Huang, Z., & Dai, J. (2014). Mechanism of Cu(II) adsorption inhibition on biochar by its aging process. *Journal Environmental Science, 26*, 2123–2130.

Hefne, J. A., Mekhemer, W. K., Alandis, N. M., Aldayel, O. A., & Alajyan, T. (2008). Kinetic and thermodynamic study of the adsorption of Pb(II) from aqueous solution to the natural and treated bentonite. *International Journal of Physical Sciences, 3*(11), 281–288.

Hovsepyan, A., & Bonzongo, J. C. J. (2009). Aluminum drinking water treatment residuals (Al-WTRs) as sorbent for mercury: implications for soil remediation. *Journal of Hazardous Materials, 164*, 73–80.

Inyang, M. I., Gao, B., Yao, Y., Xue, Y. W., Zimmerman, A., Mosa, A., et al. (2016). A review of biochar as a low-cost adsorbent for aqueous heavy metal removal. *Critical Reviews in Environmental Science and Technology, 46*(4), 406–433.

Komárek, M., Vanek, A., & Ettler, V. (2013). Chemical stabilization of metals and arsenic in contaminated soils using oxides-a review. *Environmental Pollution, 172*, 9–22.

Kuppusamy, S., Thavamani, P., & Megharaj, M. (2016). Agronomic and remedial benefits and risks of applying biochar to soil: Current knowledge and future research directions. *Environmental International, 87*, 1–12.

Liu, T., Liu, B., & Zhang, W. (2014). Nutrient and heavy metals in biochar produced by sewage sludge pyrolysis: Its application in sol amendment. *Polish Journal Environmental Study, 23*, 271–275.

Lu, S. G., & Xu, Q. F. (2009). Competitive adsorption of Cd, Cu, Pb and Zn by different soils of Eastern China. *Environmental Geology, 57*, 685–693.

Lu, H. L., Zhang, W. H., Yang, Y. X., Huang, X. F., Wang, S. Z., & Qiu, R. L. (2012). Relative distribution of Pb^{2+} sorption mechanisms by sludge-derived biochar. *Water Resource, 46*, 854–862.

Marzal, P., Seco, A., & Gabaldon, C. (1996). Cadmium and zinc adsorption onto activated carbon: influence of temperature, pH and metal/carbon ratio. *Journal Chemical Technology and Biotechnology, 66*, 279–285.

Mohan, D., & Singh, K. P. (2002). Single- and Multi-component adsorption of cadmium and zinc using activated carbon derived from bagasse—an agricultural waste. *Water Resource, 36*, 2304–2318.

Naseem, R., & Tahir, S. S. (2001). Removal of Pb(II) from aqueous/acidic solutions by using bentonite as an adsorbent. *Water Research, 35*(16), 3982–3986.

Qian, L., & Chen, B. (2013). Dual role of biochars as adsorbents for aluminum: The effects of oxygen-containing organic

components and the scattering of silicate particles. *Environmental Science and Technology, 47*, 8759–8768.

Rees, F., Simonnot, M. O., & Morel, J. L. (2014). Short-term effects of biochar on soil heavy metal mobility are controlled by intra-particle diffusion and soil pH increase. *European Journal Soil Science, 65*, 149–161.

Rorff, A. A., Elzinga, E. J., Reeder, R. J., & Fisher, N. S. (2006). The effect of aging and pH on Pb(II) sorption processes at the calcite-water interface. *Environmental Science and Technology, 40*, 1792–1798.

Song, X. D., Xue, X. Y., Chen, D. Z., He, P. J., & Dai, X. H. (2014). Application of biochar from sewage sludge to plant cultivation: Influence of pyrolysis temperature and biochar-to-soil ratio on yield and heavy metal accumulation. *Chemosphere, 109*, 213–220.

Tan, X. F., Liu, Y. G., Zeng, G. M., Wang, X., Hu, X. J., Gu, Y. L., et al. (2015). The application of biochar for the removal of pollutants from aqueous solutions. *Chemosphere, 125*, 70–85.

Tessier, A., Campbell, P. G. C., & Bisson, M. (1979). Sequential extraction procedure for the speciation of particulate trace metals. *Analytical Chemistry, 51*, 844–851.

Tong, X., Li, J., Yuan, J., & Xu, R. (2011). Adsorption of Cu(II) by biochars generated from three crop straws. *Chemical Engineering Journal, 172*, 828–834.

Tsang, D. C. W., Hu, J., Liu, M. Y., Zhang, W., Lai, K. C. K., & Lo, I. M. C. (2007). Activated carbon produced from waste wood pallets: Adsorption of three classes of dyes. *Water, Air, and Soil pollution, 184*, 141–155.

Tsang, D. C. W., & Lo, I. M. C. (2006). Competitive Cu and Cd sorption and transport in soils: A combined batch kinetics, column and sequential extraction study. *Environmental Science and Technology, 40*, 6655–6661.

Tsang, D. C. W., Olds, W. E., Weber, P. A., & Yip, A. C. K. (2013). Soil stabilisation using AMD sludge, compost and lignite: TCLP leachability and continuous acid leaching. *Chemosphere, 93*, 2839–2847.

Wesenbeeck, S. V., Prins, W., Ronsse, F., & Antal, M. J., Jr. (2014). Sewage sludge carbonization for biochar applications: fate of heavy metals. *Energy & Fuels, 28*, 5318–5326.

Zaman, M. I., Mustafa, S., Khan, S., & Xing, B. (2009). Effect of phosphate complexation on Cd^{2+} sorption by manganese dioxide (β-MnO2). *Journal of Colloid Interface Science, 330*, 9–19.

Zhang, W. H., Huang, H., Tan, F. F., Wang, H., & Qiu, R. L. (2010). Influence of EDTA-washing on the species and mobility of heavy metals residual in soils. *Journal of Hazardous Materials, 173*, 369–376.

Zhang, W. H., Mao, S. Y., Chen, H., Huang, L., & Qiu, R. L. (2013). Pb(II) and Cr(VI) sorption by biochars pyrolyzed from the municipal wastewater sludge under different heating conditions. *Bioresource technology, 147*, 545–552.

Zhang, W. H., Zheng, P., Zheng, J., Tsang, D. C. W., & Qiu, R. L. (2015). Sludge-derived biochar for arsenic(III) immobilization: Effects of solution chemistry on sorption behavior. *Journal of Environmental Quality, 44*, 1119–1126.